

WHY ATENS ENJOY ENHANCED ACCESSIBILITY FOR HUMAN SPACE FLIGHT

Daniel R. Adamo* and Brent W. Barbee†

Near-Earth objects can be grouped into multiple orbit classifications, among them being the Aten group, whose members have orbits crossing Earth's with semi-major axes less than 1 astronomical unit. Atens comprise well under 10% of known near-Earth objects. This is in dramatic contrast to results from recent human space flight near-Earth object accessibility studies, where the most favorable known destinations are typically almost 50% Atens. Geocentric dynamics explain this enhanced Aten accessibility and lead to an understanding of where the most accessible near-Earth objects reside. Without a comprehensive space-based survey, however, highly accessible Atens will remain largely unknown.

INTRODUCTION

In the context of human space flight (HSF), the concept of near-Earth object (NEO) accessibility is highly subjective (Reference 1). Whether or not a particular NEO is accessible critically depends on mass, performance, and reliability of interplanetary HSF systems yet to be designed. Such systems would certainly include propulsion and crew life support with adequate shielding from both solar flares and galactic cosmic radiation. Equally critical architecture options are relevant to NEO accessibility. These options are also far from being determined and include the number of launches supporting an HSF mission, together with whether consumables are to be pre-emplaced at the destination.

Until the unknowns of HSF to NEOs come into clearer focus, the notion of *relative* accessibility is of great utility. Imagine a group of NEOs, each with nearly equal HSF merit determined from their individual characteristics relating to crew safety, scientific return, resource utilization, and planetary defense. The *more* accessible members of this group are more likely to be explored first.

A highly accessible NEO could conceivably be deferred in favor of a less accessible HSF destination because the latter is more accessible during a programmatically desirable launch season. Such a season is really yet another undetermined HSF architecture option. A launch season's duration will likely be measured in weeks, and it will be utilized at an indeterminate point almost certainly more than a decade in the future when HSF programmatic maturity is sufficient.

Furthermore, current knowledge of the NEO population relevant to HSF is far from complete. In the 100-m-diameter class of greatest interest, only a few percent of the estimated NEO population is known (Reference 2, Figure 2.4). Therefore, any known, lost, or fictitious NEO in a highly accessible orbit is a potential HSF destination of merit. Even if lost, fictitious, small, or hazardous, such a *potential* target (or another in a similar orbit) may ultimately prove to be an early HSF destination when the pertinent NEO population is more thoroughly catalogued and NEO orbits are more thoroughly maintained at high accuracy.

* Independent Astrodynamics Consultant, 4203 Moonlight Shadow Court, Houston, TX 77059; adamod@earthlink.net.

† Aerospace Engineer, Code 595, 8800 Greenbelt Road, Greenbelt MD 20771.

This paper first reviews methodology and pertinent results from NASA-sponsored research performed in late 2010 and dubbed NEO HSF Accessible Targets Study (NHATS, pronounced as "gnats"). A useful accessibility metric developed during this study is n , the tally of NHATS-compliant mission trajectory solutions detected in association with a specific NEO. The known NEO population is then surveyed to illustrate in which regions of heliocentric semi-major axis, eccentricity, and inclination (a, e, i) space NEOs with large n values are mapped. The (a, e, i) mapping is also formatted such that membership in each of four NEO orbit classifications, as defined below, is evident.

Amors have orbits everywhere superior to (outside of) Earth's. An Amor is therefore defined to have perihelion between 1.017 astronomical units (AU) and the maximum NEO value of 1.3 AU. As of 0 hrs Universal Time on 1 January 2011 (UT epoch 2011.0), Amors numbered 2855 in the Jet Propulsion Laboratory (JPL) Small-Body Database (SBDB)*, comprising 37.7% of known NEOs.

Apollos have orbits crossing Earth's with periods greater than Earth's. An Apollo is therefore defined to have perihelion less than 1.017 AU and a greater than 1.0 AU. As of 2011.0 UT, Apollos numbered 4080 in the SBDB, comprising 53.9% of known NEOs.

Atens have orbits crossing Earth's with periods less than Earth's. An Aten is therefore defined to have aphelion greater than 0.983 AU and a less than 1.0 AU. As of 2011.0 UT, Atens numbered 618 in the SBDB, comprising 8.2% of known NEOs.

Atiras have orbits everywhere inferior to (inside of) Earth's. An Atira is therefore defined to have aphelion less than 0.983 AU. As of 2011.0 UT, Atiras numbered 11 in the SBDB, comprising 0.1% of known NEOs.

It is no surprise that the largest n values are chiefly associated with Apollos and Atens. Because these orbits cross Earth's, distance to be covered in a given round trip mission time Δt can be far less than is possible for Amors or Atiras (Reference 1, Figure 7). This Δt or the sum of mission propulsive impulse magnitudes Δv can more frequently be minimized to enhance NHATS compliance for Apollos and Atens than is generally the case for Amors and Atiras.

A less intuitive trend in NHATS results is that Atens nearly outnumber the more numerous Apollos among the most compliant NEOs as measured by n . This trend is completely out of proportion to the degree Atens are represented among the known NEO population. A theory based on geocentric NEO relative motion is presented by this paper to explain why Atens enjoy inherently greater accessibility than do Apollos.

Another trend evident from mapping into (a, e, i) space is the dearth of known NEOs at low e when $a < 1$ AU. Underrepresentation of Atens and Atiras in the NEO catalog is at least in part attributable to observing exclusively from a perspective near Earth (Reference 2, pp. 41-49). Generally inferior Aten and Atira orbits are rarely, if ever, in Earth's night sky (Reference 2, Figure 3.5). Until a comprehensive NEO survey is conducted from an appropriate region remote from Earth, the theory developed in this paper indicates a substantial fraction of the most accessible NEOs will remain unknown. The accessibility theory developed in this paper has the potential to offer guidance in design, deployment, and operation of this survey.

PERTINENT NHATS TECHNIQUES AND RESULTS

Inaugurated by NASA in August 2010, NHATS is conceived as a means to assess the proliferation of *potential* NEO destinations accessible for HSF. Data with a NHATS pedigree reported in this paper have undergone thorough technical review by two independent research teams and are considered accurate in the context of that study's assumptions and constraints. However, readers should understand NHATS data are being disclosed in the interest of technical interchange before NASA has made any HSF architecture or NEO destination decisions based on this research. Until these decisions are made, whether or not a specific

* The SBDB may be accessed via a search engine at http://ssd.jpl.nasa.gov/sbdb_query.cgi or via a browser at <http://ssd.jpl.nasa.gov/sbdb.cgi> [verified 1 January 2011].

NHATS-viable NEO is accessible for HSF remains an open question. The following two sub-sections report NHATS assessment techniques and results internally reviewed and adopted by NASA prior to November 2010.

Constraints, Computations, And Criteria Identifying Viable NHATS Destinations

To be considered a viable destination under NHATS criteria, a NEO is required to be associated with at least one compliant trajectory design. Every NEO catalogued in the SBDB as of UT epoch 1.0 September 2010 (a total of 7210 with 2718 or 37.7% being Amors, 3893 or 54.0% being Apollos, 589 or 8.2% being Atens, and 10 or 0.1% being Atiras) is evaluated for compliant trajectory designs under NHATS ground rules. The trajectory design Earth departure interval (EDI) is confined to *Horizons*-internal coordinate time (CT) epochs from 1.0 January 2015 to 31.0 December 2040 to keep the evaluation task HSF-relevant and computationally manageable. *Horizons* is JPL's on-line solar system data and ephemeris computation service (Reference 3) and may be accessed at <http://ssd.jpl.nasa.gov/?horizons> [verified 29 December 2010].

Barbee et al document in detail the method of embedded trajectory grids used to compute NHATS trajectory designs (Reference 4). Each design consists of three segments.

The first *outbound* segment is a heliocentric conic trajectory departing Earth and arriving at the NEO destination during time interval Δt_1 such that $4 \text{ days} \leq \Delta t_1 \leq 358 \text{ days}$. The 2-dimensional array (or grid) of NHATS-permissible outbound segment EDI epochs (columns) is incremented at 6-day intervals, as are associated Δt_1 values (rows). Outbound segment departure is from a circular Earth parking orbit of geocentric radius r_{EPO} (equivalent to an orbit height 400 km above Earth's equatorial radius r_E) and requires an impulsive change-in-velocity magnitude at trans-NEO injection of Δv_{TNI} . Patched conic theory is used to compute Δv_{TNI} from the outbound segment's required Earth departure energy C_3 and Earth's reduced mass μ_E as follows.

$$\Delta v_{TNI} = \sqrt{C_3 + \frac{2 \mu_E}{r_{EPO}}} - \sqrt{\frac{\mu_E}{r_{EPO}}}$$

The second *loiter* segment matches the NEO destination's trajectory as defined by *Horizons* during time interval Δt_2 between NEO arrival and departure such that $8 \text{ days} \leq \Delta t_2 \leq 40 \text{ days}$. To initiate loiter at the end of the outbound trajectory segment, an impulsive change-in-velocity magnitude of Δv_A is required at NEO destination arrival.

The third *return* segment is a heliocentric conic trajectory departing the NEO destination and arriving at Earth atmospheric entry interface during time interval Δt_3 such that $4 \text{ days} \leq \Delta t_3 \leq 358 \text{ days}$. A return segment grid of departure/arrival epochs is embedded at each element of the outbound segment's grid. The embedded grid consists of return segment NEO departure epochs (columns) incremented at 2-day intervals and associated Δt_3 values (rows) incremented at 6-day intervals. To initiate return following loiter, an impulsive change-in-velocity magnitude of Δv_D is required at NEO destination departure. A return trajectory segment is defined to arrive at a geocentric radius of r_{EI} (defined to be at a height 121.92 km above r_E) and is further constrained to a geocentric speed no more than $v_{EIX} = 12.5 \text{ km/s}$ at that arrival point. Coasted geocentric Earth atmospheric entry interface speed v_{EI} is computed from geocentric asymptotic Earth return segment speed v_∞ using patched conic theory as follows.

$$v_{EI} = \sqrt{v_\infty^2 + \frac{2 \mu_E}{r_{EI}}}$$

In cases where $v_{EI} > v_{EIX}$, an atmospheric braking impulse magnitude $\Delta v_{EI} = v_{EI} - v_{EIX}$ is computed. Otherwise, no such impulse is necessary and $\Delta v_{EI} = 0$.

Multiple criteria must be satisfied for a trajectory design to be deemed NHATS-compliant. First, $\Delta t = \Delta t_1 + \Delta t_2 + \Delta t_3$ must not exceed 365 days to maintain radiation and microgravity exposure risks to the crew at reasonable levels. Second, C_3 must not exceed $24 \text{ km}^2/\text{s}^2$ to maintain reasonable propulsive performance expectations at Earth departure when vehicle mass is likely greatest during the three trajectory design seg-

ments. Third, $\Delta v = \Delta v_{TNI} + \Delta v_A + \Delta v_D + \Delta v_{EI}$ must not exceed 12 km/s to maintain reasonable propulsive performance expectations throughout the HSF mission.

Readers familiar with current interplanetary HSF capabilities will find the foregoing NHATS trajectory design constraints and compliance criteria to border on the realm of science fiction in multiple respects. This astronautic optimism might be excessive even if reasonable state-of-the-art progress through the 2030s is assumed. Such optimism is intentional. A major NHATS objective is to determine whether or not a dedicated space-based survey is justified by the proliferation of known NEO destinations available for HSF missions. Initial NHATS compliancy processing documented here is therefore biased toward inclusion. Subsequently, NASA plans to cull this initial list of potential NEO destinations using other considerations such as physical characteristics (size, composition, spin, etc.), orbit prediction uncertainty, and accessibility with respect to HSF infrastructure capabilities during specific Earth departure seasons.

Viable NHATS Destinations With Maximum Trajectory Design Compliance

Selecting NEO HSF destinations from a known population whose physical characteristics are largely unknown is well beyond the scope of this paper. Furthermore, as noted in the Introduction, the known NEO population is but an observationally biased sample amounting to only a few percent of the whole at HSF-relevant diameters near 100 m.

In contrast to *selecting* NEO destinations for HSF (literally in the blind), *ranking* them according to their compliance with NHATS trajectory design criteria is very useful at this point. At the very least, this ranking exercise identifies a subset of known NEO orbits highly accessible for HSF. As NEO surveys continue under mandates from the U.S. Congress (Reference 2, p. 1), identifying orbit classes of higher interest will lead to more informed and cost-effective observation strategies. For example, inability to detect NEOs approaching Earth from the Sun's general direction could easily rule out 50% of all HSF mission opportunities simply because such opportunities will not be evident with sufficient time to prepare for launch.

Processing under constraints and compliance criteria outlined in the previous section has identified 666 NEOs with at least one NHATS-compliant trajectory design. Of these, 106 (15.9%) are Amors, 390 (58.6%) are Apollos, 170 (25.5%) are Atens, and none are Atiras. But a handful of barely viable trajectories over the 26-year NHATS EDI cannot qualify a potential destination as highly accessible, particularly in the context of intentionally inclusive NHATS trajectory design constraints and compliance criteria.

Table 1 ranks viable NHATS destinations in order of decreasing n , the total number of compliant trajectory solutions associated with each destination. Only the top 50 NEOs according to this ranking are included, rendering Table 1 a plausible list of the most accessible NHATS destinations. Very little characterization data are available for Table 1 NEOs, but a range of likely diameter d values in meters is provided using the following relationship based on absolute magnitude H and a likely range of albedo values ρ ranging from 0.05 to 0.25.

$$d = \frac{1,329,000}{\sqrt{\rho}} 10^{-0.2H}$$

Osculating heliocentric orbit elements appearing in Table 1 (a is semi-major axis, e is eccentricity, and i is ecliptic inclination) are from the SBDB as configured 3 January 2011.

Table 1. The 50 Most Accessible NHATS Destinations Ranked According to n .

Rank	Designation	n	Likely d (m)	a (AU)	e	i (deg)	Orbit Group
1	2000 SG ₃₄₄	4,153,445	29 to 66	0.977	0.067	0.1	Aten
2	1991 VG	3,524,012	6 to 12	1.027	0.049	1.4	Apollo
3	2008 EA ₉	2,189,719	8 to 17	1.059	0.080	0.4	Apollo
4	2001 FR ₈₅	1,991,566	33 to 75	0.983	0.028	5.2	Aten
5	2006 BZ ₁₄₇	1,845,936	22 to 49	1.024	0.099	1.4	Apollo
6	2007 UN ₁₂	1,836,008	5 to 11	1.054	0.060	0.2	Apollo
7	2008 HU ₄	1,778,197	6 to 13	1.093	0.073	1.3	Apollo
8	2006 RH ₁₂₀	1,687,566	3 to 7	1.033	0.025	0.6	Apollo

Rank	Designation	<i>n</i>	Likely <i>d</i> (m)	<i>a</i> (AU)	<i>e</i>	<i>i</i> (deg)	Orbit Group
9	2008 UA ₂₀₂	1,419,978	3 to 8	1.033	0.068	0.3	Apollo
10	2007 VU ₆	1,393,440	13 to 29	0.976	0.091	1.2	Aten
11	2004 QA ₂₂	1,342,378	7 to 16	0.951	0.122	0.6	Aten
12	2009 BD	1,225,392	6 to 13	1.002	0.047	0.4	Apollo
13	1999 VX ₂₅	1,204,010	12 to 27	0.900	0.140	1.7	Aten
14	2001 GP ₂	1,124,586	11 to 25	1.038	0.074	1.3	Apollo
15	2008 JL ₂₄	1,100,888	3 to 7	1.038	0.107	0.5	Apollo
16	2000 SZ ₁₆₂	1,018,474	10 to 23	0.930	0.168	0.9	Aten
17	2004 VJ ₁	1,017,841	37 to 83	0.944	0.164	1.3	Aten
18	2010 JR ₃₄	1,011,306	8 to 17	0.960	0.145	0.7	Aten
19	2009 OS ₅	993,890	51 to 115	1.144	0.097	1.7	Amor
20	2007 YF	892,078	30 to 66	0.953	0.120	1.7	Aten
21	1993 HD	882,148	20 to 45	1.126	0.040	0.5	Amor
22	2000 LG ₆	869,476	4 to 9	0.917	0.111	2.8	Aten
23	2009 YR	860,265	7 to 15	0.942	0.110	0.7	Aten
24	2001 QJ ₁₄₂	800,937	55 to 123	1.062	0.086	3.1	Apollo
25	2009 YF	794,499	31 to 69	0.936	0.121	1.5	Aten
26	2006 DQ ₁₄	785,949	10 to 23	1.028	0.053	6.3	Apollo
27	1999 CG ₉	784,795	25 to 55	1.060	0.063	5.2	Apollo
28	1999 AO ₁₀	771,044	45 to 101	0.912	0.111	2.6	Aten
29	2008 DL ₄	756,226	11 to 26	0.929	0.123	3.2	Aten
30	2005 LC	743,975	12 to 26	1.133	0.102	2.8	Amor
31	2008 ST	736,888	10 to 23	0.964	0.126	1.9	Aten
32	2010 JK ₁	687,496	36 to 79	1.026	0.150	0.2	Apollo
33	2003 SM ₈₄	685,501	76 to 169	1.126	0.082	2.8	Amor
34	2005 UV ₆₄	682,372	13 to 28	0.958	0.116	5.4	Aten
35	2003 WT ₁₅₃	676,727	7 to 15	0.894	0.178	0.4	Aten
36	2009 CV	641,350	37 to 84	1.112	0.150	1.0	Apollo
37	2006 UQ ₂₁₆	631,360	9 to 21	1.104	0.162	0.5	Apollo
38	2001 BB ₁₆	606,609	80 to 179	0.854	0.172	2.0	Aten
39	2009 DB ₄₃	589,918	14 to 30	1.102	0.172	0.9	Apollo
40	2008 CX ₁₁₈	582,718	35 to 78	1.145	0.035	2.4	Amor
41	2007 BB	564,165	7 to 16	0.932	0.142	3.5	Aten
42	2009 HC	557,435	30 to 66	1.039	0.126	3.8	Apollo
43	2006 UB ₁₇	557,021	15 to 33	1.141	0.104	2.0	Amor
44	2004 JN ₁	531,561	54 to 121	1.085	0.176	1.5	Apollo
45	2007 XB ₂₃	525,765	10 to 23	1.041	0.054	8.5	Apollo
46	2009 UD	503,677	10 to 22	1.038	0.121	4.4	Apollo
47	2006 FH ₃₆	480,108	69 to 155	0.955	0.198	1.6	Aten
48	2008 EL ₆₈	448,257	7 to 15	1.210	0.192	0.6	Apollo
49	2008 CM ₇₄	432,970	7 to 15	1.089	0.147	0.9	Apollo
50	2007 RC ₂₀	430,820	13 to 28	0.955	0.198	2.8	Aten

The Table 1 breakdown according to orbit groups is 6 Amors (12.0%), 23 Apollos (46%), 21 Atens (42%), and no Atiras (0%). Compare the ratio of Apollos-to-Atens in Table 1 (23/21 = 1.095) to that in the SBDB processed by NHATS (3893/589 = 6.610). It is not intuitively obvious why this 6-fold selectivity should apply to Atens in the context of relatively high HSF accessibility. A theory applying geocentric relative motion to heliocentric NEO orbits is presented subsequently to provide an understanding of this selectivity.

Another noteworthy trend in Table 1 is that no *i* value exceeds 10°. When the entire list of 666 viable NHATS destinations is scanned for *i* > 10° members, the highest ranking is the 189th, 2007 VV₈₃, with a diminutive *n* = 54,819. A necessary condition for high accessibility among NEOs is evidently *i* < 10°.

The 50 most accessible NEOs identified by Table 1 are annotated in Figure 1, including their rank according to n . In the interest of legibility, NEO designations in Figure 1 annotations refrain from using subscripted numerals. Thus, the NEO with highest n -ranking is annotated as "2000 SG344 #1" in Figure 1.

Two NEOs not appearing in Table 1 are annotated in Figure 1. The first of these is (99942) Apophis at (a, e, i) coordinates (0.922 AU, 0.191, 3.3°). With $d = 270$ m, Apophis will become the largest NEO to encounter Earth so closely when it reaches a predicted perigee radius of 38,000 km on 13 April 2029. Because of this event, both robotic and HSF mission proposals targeting Apophis are prolific. With $n = 204,028$, however, Apophis is ranked #101 among viable NHATS destinations. Particularly when inadvertent changes to future Earth collision prospects are considered, visiting Apophis early in a NEO exploration program is ill advised. There are many more accessible and less potentially hazardous destinations warranting a visit before Apophis is considered.

The second NEO annotated in Figure 1, but absent from Table 1, is 2003 YN₁₀₇. At (a, e, i) coordinates (0.989 AU, 0.014, 4.3°), 2003 YN₁₀₇ is in the most Earth-like orbit of any known NEO as of 2011.0 UT. This attribute ought to rank 2003 YN₁₀₇ among the most accessible NHATS destinations, but its Figure 1 annotation has no rank because its n is zero. The reason 2003 YN₁₀₇ is excluded as a viable NHATS destination lies with its synodic period t_s .

Provided a NEO of interest undergoes no close planetary encounters during an interval of interest, t_s can be computed with sufficient accuracy from NEO and Earth mean heliocentric orbit rates (ω and ω_R , respectively) as follows. Using the Sun's reduced mass μ_S , orbit rates derive directly from Kepler's third law (the square of orbit period is proportional to the cube of semi-major axis). Earth's semi-major axis in Equation (2) is approximated by $a_R = 1$ AU.

$$\omega = \sqrt{\frac{\mu_S}{a^3}} \quad (1)$$

$$\omega_R = \sqrt{\frac{\mu_S}{a_R^3}} \quad (2)$$

Synodic period is the time required for orbit rate difference to sweep out a full revolution such that the NEO "laps" Earth or vice-versa.

$$t_s = \frac{2\pi}{|\omega - \omega_R|} \quad (3)$$

In the case of 2003 YN₁₀₇, $a = 0.989$ AU. When Equations (1) and (3) are evaluated for 2003 YN₁₀₇, the synodic period is 61.6 Julian years. This t_s greatly exceeds the 26-year period during which NHATS missions lasting less than one year must be initiated. It is therefore evident that 2003 YN₁₀₇ has slowly *phased ahead* of Earth (the Earth-Sun-NEO phase angle θ has increased from zero) since its late 2003 discovery to an extent inhibiting any NHATS-compatible trajectory during the required 1.0 January 2015 to 31.0 December 2040 UT EDI.

To indicate that portion of Figure 1 in which NEOs would have $t_s > 25$ Julian years, the plot is accompanied by two vertical loci of constant semi-major axis. The first locus is positioned inferior to a_R at a_I , and the second locus is positioned superior to a_R at a_S . Thus, the two loci bracket all Figure 1 NEOs having $t_s > 25$ Julian years. Semi-major axis values for these loci are obtained by substituting Equation (1) into Equation (3) and solving for a while ensuring the difference in orbit rate from Equation (3)'s denominator is maintained positive ($\omega - \omega_R$ for the inferior case and $\omega_R - \omega$ for the superior case) without computing an absolute value.

$$a_I = \left[\mu_S / \left(\omega_R + \frac{2\pi}{t_s} \right)^2 \right]^{1/3} \quad (4)$$

$$a_s = \left[\mu_s / \left(\omega_R - \frac{2\pi}{t_s} \right)^2 \right]^{1/3} \quad (5)$$

When evaluated for $t_s = 25$ Julian years, Equation (4) produces $a_I = 0.974191$ AU, and Equation (5) produces $a_S = 1.027589$ AU. Note the slight asymmetry of a_I and a_S about $a_R = 1$ AU. Here is the first of four inferior/superior asymmetries documented in this paper, and they all relate to enhanced accessibility among Atens. In effect, a broader range of orbit rates exists over a given a increment *inferior* to Earth's orbit than is present over the same increment *superior* to Earth's orbit.

It is a straightforward exercise to compute heliocentric phasing of 2003 YN₁₀₇ with respect to Earth during the NHATS EDI from 1.0 January 2015 to 31.0 December 2040 UT and thereby explain the $n = 0$ result for this NEO. Phasing over this interval is shown graphically in Figure 2 by mapping the heliocentric 2003 YN₁₀₇ *Horizons* ephemeris into the Cartesian UVW coordinate system defined by Earth's heliocentric *Horizons* ephemeris using a 30-day time increment.

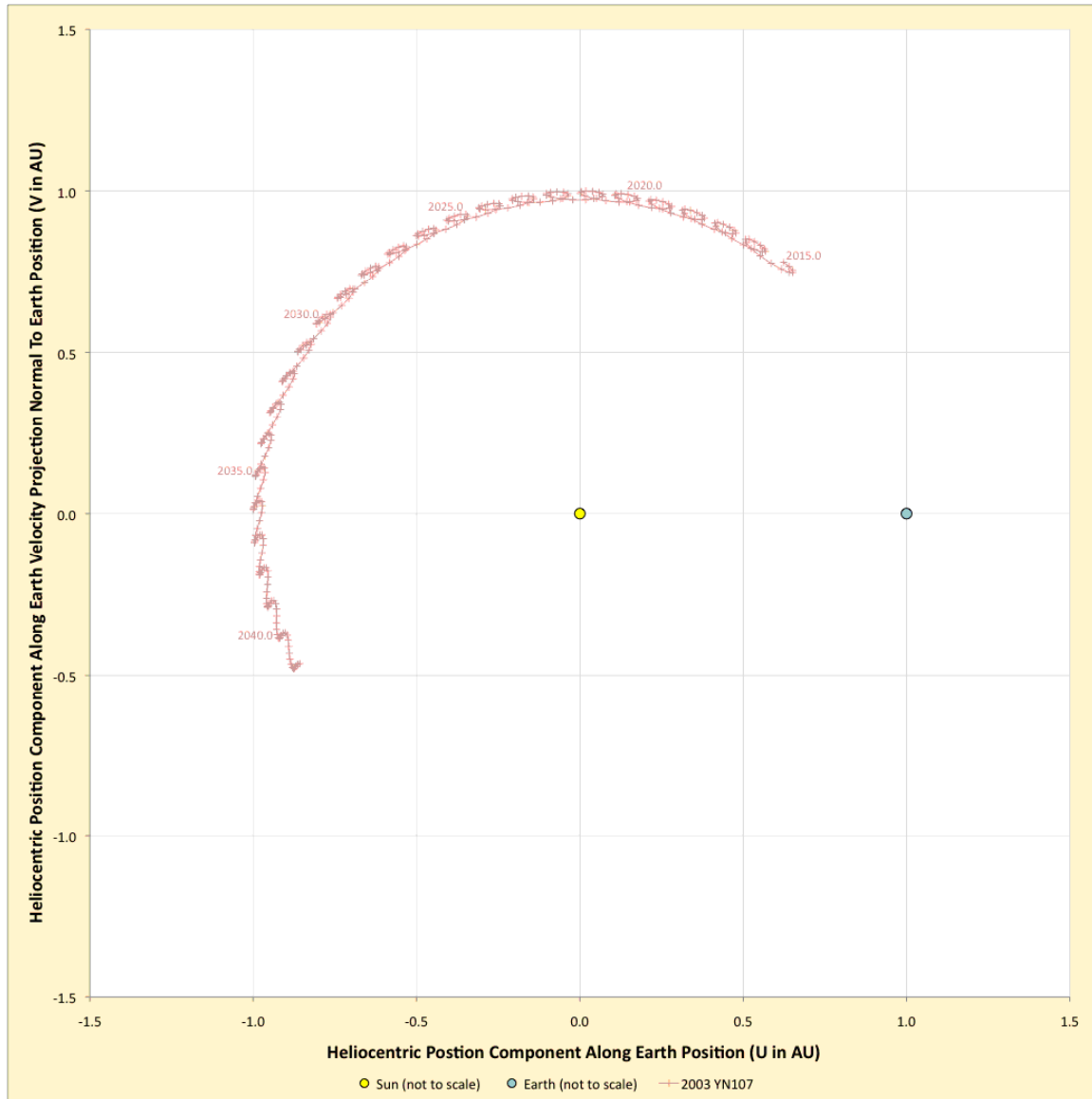


Figure 2. Heliocentric UV Plot of 2003 YN₁₀₇ Phasing During The NHATS EDI.

In Figure 2's context, the unit vector U is aligned with Earth's heliocentric position, W is aligned with Earth's heliocentric angular momentum vector, and $U \times V = W$ in the right-handed convention. Because Figure 2 is confined to Earth's orbit plane, it is called a heliocentric UV plot. In such a plot, Earth is fixed at heliocentric (U, V) coordinates (1, 0) AU. A NEO whose position is phased ahead of Earth (with $0 < \theta < 180^\circ$) has a positive V-coordinate, and one behind Earth (with $-180^\circ < \theta < 0$) has a negative V-coordinate. Figure 2's plot is annotated with 1.0 January UT epochs at 5-year intervals beginning with "2015.0". Since θ is far from zero in Figure 2, the $n = 0$ NHATS assessment for 2003 YN₁₀₇ lends further credence to the assertion that HSF mission opportunities with minimal Δt and Δv occur only during timeframes when the NEO destination encounters Earth within 0.1 AU (Reference 1).

What would be the NHATS assessment for 2003 YN₁₀₇ if Earth departures were confined to years 1997 through 2007? According to *Horizons*, this EDI around the time of 2003 YN₁₀₇ discovery contains no less than 21 perigees closer than 0.1 AU. The result of this biased departure time NHATS assessment is $n = 10,141,782$, exceeding any Table 1 value by a factor of at least 2.4 (2000 SG₃₄₄, ranked #1, has $n = 4,153,445$). The high *intrinsic* accessibility of 2003 YN₁₀₇, as apparent from Figure 1, is confirmed.

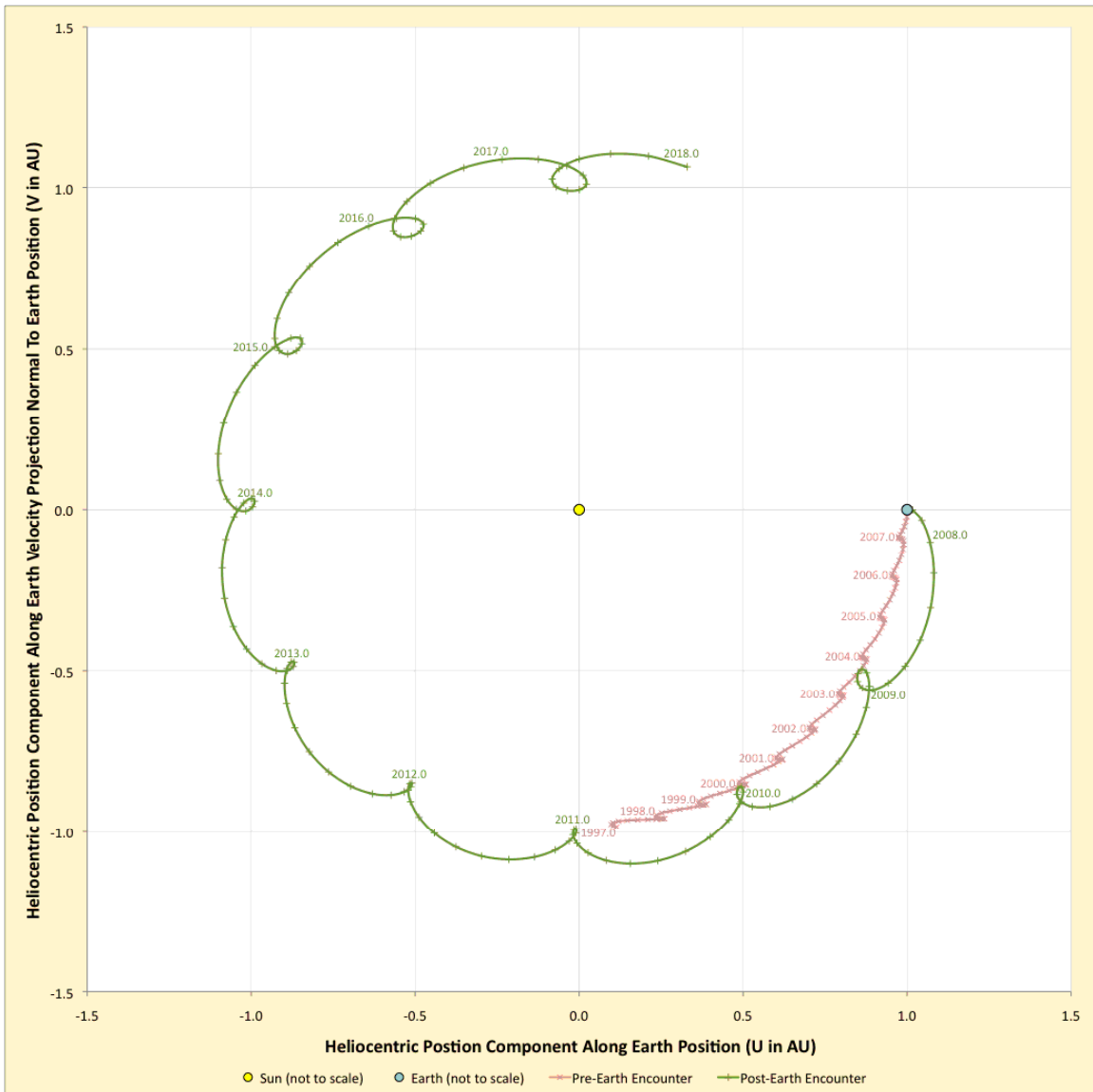


Figure 3. Heliocentric UV Plot of 2007 UN₁₂ Transformation from an Aten to an Apollo.

A noteworthy feature of (a, e, i) plots like Figure 1's is that some NEOs undergo dramatic coordinate shifts over time scales of months or less. Such events typically occur during a close Earth encounter and may therefore be associated with a NEO's discovery or an HSF mission opportunity. An example of dramatic (a, e, i) dynamics is provided by 2007 UN₁₂, whose Table 1 rank is #6. During the timeframe of this NEO's discovery, it encountered Earth with a perigee less than 0.000467 AU (69,900 km) on 17.6 October 2007 UT according to *Horizons*. In terms of (a, e, i) coordinates from *Horizons*, 2007 UN₁₂ went from (0.992 AU, 0.010, 3.080°) on 17.0 September 2007 UT to (1.053 AU, 0.061, 0.236°) 60 days later on 16.0 November 2007 UT. As illustrated in Figure 3's UV plot, Earth gravity perturbations to the 2007 UN₁₂ orbit during 2007 transformed it from that of an Aten to that of an Apollo.

As of Figure 1's 2011.0 UT osculation epoch, a series of six close Earth approaches begun in 2008 is nearing completion for 2009 BD at $(a, e, i) = (1.004 \text{ AU}, 0.046, 0.374^\circ)$. By the earliest NHATS Earth departure epoch at 1.0 January 2015 CT, *Horizons* predicts 2009 BD's coordinates will have shifted to (1.062 AU, 0.052, 1.267°), well clear of the $t_S > 25$ years region in Figure 1. Of all Table 1 NEOs, 2009 BD's coordinates are by far the most dynamic over the interval from 2011.0 to 2042.0 CT, but only 2.6% of 2009 BD a variations during this interval occur after 2012.0 CT. Indeed, all Table 1 NEOs exhibit remarkably static a values during the NHATS assessment interval. At no time during this interval does a superior Table 1 NEO become inferior, nor does an inferior NEO become superior.

A THEORY OF NEO ACCESSIBILITY DYNAMICS FOR HSF

With HSF missions constrained to be round trips lasting well under a year, NEO accessibility must place a premium on minimal distance between Earth and destination in the mission timeframe. As recently documented (Reference 1), this precept has its basis in the simple "distance equals rate times time" relationship. At a given NEO distance, minimal rate (and minimal propulsive mass) generally requires maximum mission duration. Likewise, at a given mission duration, minimal propulsive mass generally requires minimal NEO distance. From the utility of (a, e, i) plots demonstrated in the previous section, a question naturally arises. Where on such plots are NEO orbits with minimal separation from Earth's to be found?

To address that question, a simplifying constraint is first imposed and retained throughout this section. The constraint fixes minimal separation from Earth's heliocentric orbit at an apsis in a NEO's heliocentric orbit. Thus, Amors and Apollos will come to minimum separation at perihelion, while Atens and Atiras will come to minimum separation at aphelion under this constraint.

The perigee-at-apsis constraint is a close approximation to actual geometry for highly accessible NEOs. At 2011.0 UT, Earth's orbit would be plotted in Figure 1 at $(a, e, i) = (1.001 \text{ AU}, 0.017, 0.002^\circ)$ according to *Horizons*. Earth's orbit eccentricity is but 68% of the smallest e value appearing in Table 1 (2006 RH₁₂₀, ranked #8, has $e = 0.025$). Consequently, any NEO orbit encountering Earth's away from an apsis will possess a heliocentric radial velocity component generally far greater than Earth's at that location. This radial NEO motion is as detrimental to accessibility as motion out of the ecliptic plane previously identified in connection with i . Therefore, the best close Earth encounter geometry from the standpoint of HSF accessibility is generally parallel to Earth's heliocentric orbit and near a NEO orbit apsis.

In the ideal accessibility condition of zero perigee constrained to be at a NEO heliocentric apsis (ZePHA), geometric properties of a NEO's orbit ellipse give rise to Equation (6).

$$a_R = a (1 \pm e) \tag{6}$$

With $a > 1$ AU (Amors and Apollos), e is subtracted in Equation (6) to place NEO perihelion on Earth's orbit. With $a < 1$ AU (Atens and Atiras), e is added in Equation (6) to place NEO aphelion on Earth's orbit. A ZePHA condition is the second inferior/superior asymmetry documented in this paper. From Equation (6), $a/a_R = (1 \pm e)^{-1}$. At any given e , inferior Atens and Atiras will possess a/a_R closer to 1 AU (the semi-major axis of Earth's orbit) than the corresponding superior Amors and Apollos. Once again, accessibility of inferior NEOs is favored over superior NEOs. For the purpose of mapping a locus of ZePHA points onto an (a, e, i) plot, Equation (6) is solved for e .

$$e = \left| \frac{a_R}{a} - 1 \right| \quad (7)$$

As noted previously, NEOs such as (99942) Apophis can approach Earth very closely without being among the most accessible. The Equation (7) condition is necessary for high HSF accessibility, but it is not sufficient. A condition limiting geocentric speed is also necessary. One such condition easily mapped onto (a, e, i) plots is developed here and called the geocentric relative motion stall (GReMS). At an arbitrary heliocentric apsis distance r_X , the GReMS condition requires heliocentric tangential velocity in a NEO orbit, whose magnitude is given by the energy integral, be equal to local tangential velocity at Earth's mean orbit rate. This condition gives rise to Equation (8).

$$\sqrt{\mu_s \left(\frac{2}{r_X} - \frac{1}{a} \right)} = \omega_R r_X \quad (8)$$

Squaring both sides of Equation (8) leads to the following cubic in r_X .

$$\frac{\omega_R^2 r_X^3}{\mu_s} + \frac{r_X}{a} - 2 = 0 \quad (9)$$

The solution to this cubic can be computed as follows.

$$f_1 \equiv \frac{\omega_R^2}{\mu_s} \quad (10)$$

$$f_2 \equiv \left[9 a^3 f_1^2 + \sqrt{3 a^3 f_1^3 (27 a^3 f_1 + 1)} \right]^{1/3} \quad (11)$$

$$r_X = \frac{f_2}{9^{1/3} a f_1} - \frac{1}{3^{1/3} f_2} \quad (12)$$

With this apsis solution in hand, the GReMS eccentricity corresponding to a is computed by substitution into Equation (7).

$$e = \left| \frac{r_X}{a} - 1 \right| \quad (13)$$

Numeric results from Equations (10) through (13) relevant to highly accessible NEOs appear in Table 3 for discrete a values on Figure 1's horizontal axis. Table 3's Δr column is a heliocentric conic estimate of perigee when a NEO undergoes GReMS in the $+U$ direction with zero θ ($\Delta r \equiv |r_X - a_R|$).

Table 3. GReMS Conditions Near $a = 1$ AU.

a (AU)	r_X (AU)	Δr (AU)	e
0.80	0.938567	0.061433	0.173209
0.85	0.956401	0.043599	0.125178
0.90	0.972423	0.027577	0.080470
0.95	0.986886	0.013114	0.038828
1	1	0	0
1.05	1.011940	0.011940	0.036248
1.10	1.022852	0.022852	0.070135
1.15	1.032861	0.032861	0.101860
1.20	1.042073	0.042073	0.131605

Table 3 immediately suggests a third inferior/superior asymmetry favoring Aten and Atira HSF accessibility. At a given e , the associated GReMS condition for an inferior NEO orbit will be at an a closer to Earth's semi-major axis than the corresponding GReMS a for a superior NEO orbit. For example, an inferior NEO

with $e = 0.038828$ must have $a = 0.95$ AU to undergo GReMS at aphelion. But a superior NEO with $e = 0.038828$ must have $a > 1.05$ AU to undergo GReMS at perihelion.

A fourth asymmetry lurks in Table 3 within its rightmost two columns, but it requires mental interpolation to perceive. At a given e , the associated GReMS condition for an inferior NEO orbit will be at a smaller geocentric distance than the corresponding GReMS geocentric distance for a superior NEO orbit. This asymmetry is easily perceived when e is plotted as a function of Δr for inferior orbits and for superior orbits in Figure 4.

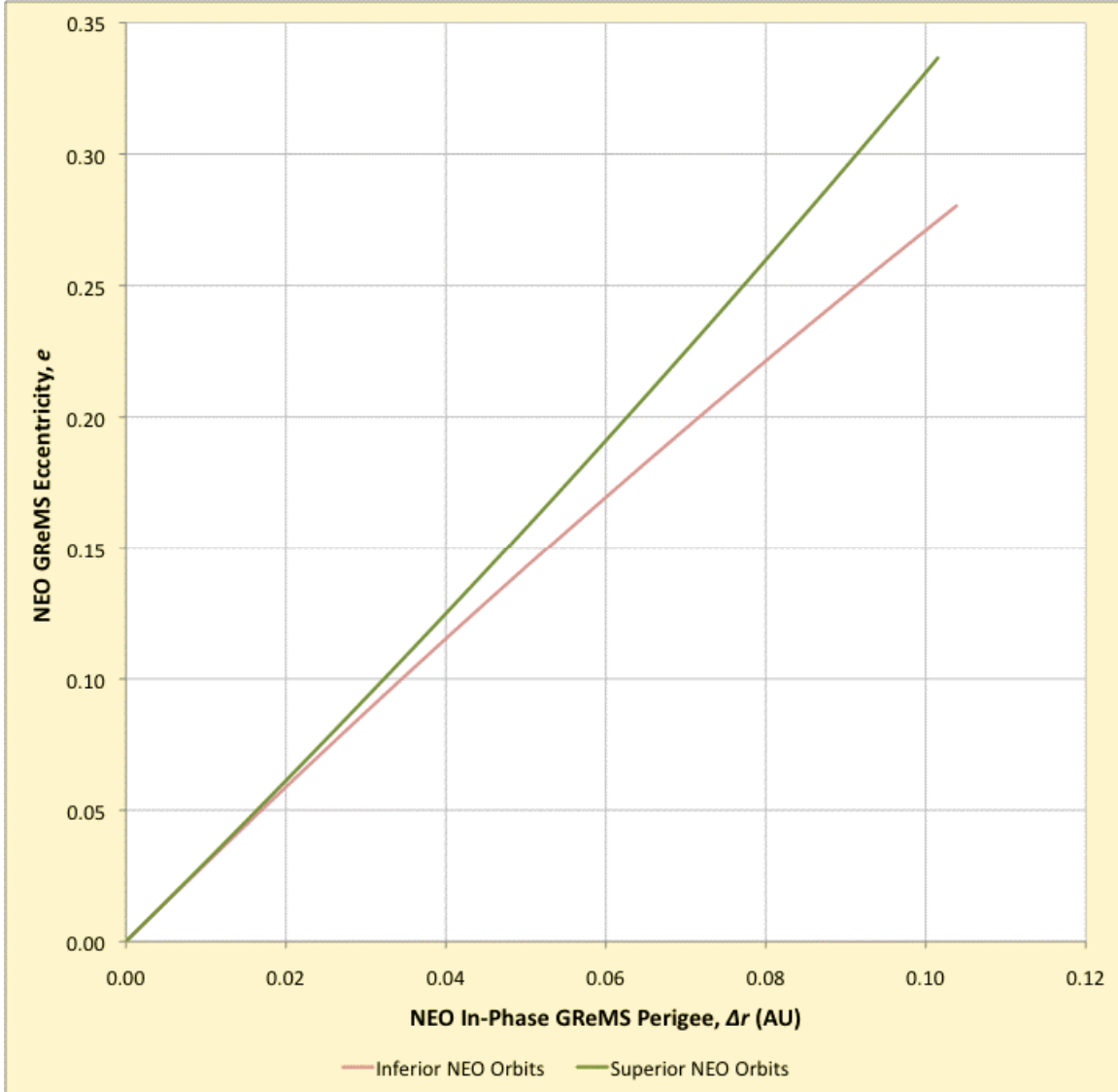


Figure 4. In-Phase GReMS Perigee Asymmetry Between Inferior & Superior NEO Orbits.

With both Table 3 asymmetries relating to e , it is important to understand their significance is undiminished by the GReMS condition's independence of e per Equations (10) through (12). This independence arises only because GReMS is defined to occur at a NEO apsis, where radial heliocentric velocity is zero. However, immediately before and after the GReMS epoch, finite radial heliocentric velocity reducing NEO accessibility *does* exist, and its negative influence *will* be enhanced according to e .

To summarize the NEO accessibility theory, a ZEPHA locus is plotted using Equation 7 and a GReMS locus is plotted using Equations 10 through 13, together with the Figure 1 data and annotations, producing

and those of NHATS destinations in Table 1? The following section details a simulation method to answer these questions.

USING FICTITIOUS NEOs TO ASSESS HSF ACCESSIBILITY THEORY

The baseline concept of creating plausible (but yet to be discovered) "fictitious" NEOs for accessibility assessment is facilitated in *Horizons* through User-Specified Small Bodies (USSBs). A variety of optional orbit element sets may be used to temporarily define a USSB in *Horizons*. Once defined, a USSB ephemeris may be generated with the same JPL Standard Dynamical Model (SDM) routinely supporting SBDB trajectory predictions by *Horizons*. A USSB ephemeris, together with JPL's DE405 for the Earth, is then exported by *Horizons* for HSF accessibility assessment using NHATS constraints, computations, and criteria previously documented. Inputs required to create fictitious NEO initial conditions as a USSB in *Horizons* are documented in the following subsection. To evaluate Figure 5's NEAR, fictitious NEO ephemerides are generated within sequences of constant (e, i) coordinates in which a is progressively increased.

Two deviations from the foregoing fictitious NEO baseline concept are necessary to evaluate HSF accessibility theory under minimally controlled conditions. First, as detailed subsequently, SDM perturbations to heliocentric conic motion introduce (a, e, i) dynamics often disrupting USSB long-term membership in a single NEO orbit classification. To maintain a controlled experimental relationship between orbit classification membership and HSF accessibility, USSB trajectory prediction with the SDM is therefore abandoned in favor of fictitious NEO conic (or Keplerian or two-body) heliocentric motion.

Second, as detailed subsequently, fictitious NEO orbit period resonances with Earth create significant variations in n with a due to the extended 1.0 January 2015 to 31.0 December 2040 CT EDI applicable to NHATS. These variations are effectively eliminated by using an EDI from 20.0 September 2025 to 18.0 September 2030 CT. Constraints, computations, and criteria attributable to NHATS and documented previously are otherwise preserved by accessibility assessments presented for fictitious NEOs.

Creating Fictitious NEO Initial Conditions In *Horizons*

The following osculating quantities, referenced to the Cartesian heliocentric ecliptic coordinate system at epoch J2000.0 (J2KE), are used to create fictitious NEO initial conditions in *Horizons*. The J2KE system is defined by \mathbf{I} directed at the ascending node of Earth's orbit plane at epoch J2000.0 on the Earth mean equatorial plane of epoch J2000.0, \mathbf{K} oriented normal to Earth's orbit plane at epoch J2000.0 (directed into the northern geocentric celestial hemisphere), and $\mathbf{J} = \mathbf{K} \times \mathbf{I}$ in the right-handed convention.

EPOCH: osculating epoch Julian ephemeris date in CT. For all fictitious NEOs, the EPOCH value is selected at a vernal equinox approximately midway through the NHATS EDI from 1.0 January 2015 to 31.0 December 2040 CT. Because J2KE elements are in use, this equinox is reckoned with respect to Earth crossing the J2KE \mathbf{I}/\mathbf{K} plane and occurs at 20.5 March 2028 CT or 2,461,851.0 Julian ephemeris date CT according to *Horizons*. In this paper's narrative, 20.5 March 2028 CT is often referred to as a fictitious NEO's initialization epoch.

EC: the value of e specific to the fictitious NEO ephemeris sequence being generated.

MA: mean anomaly in deg. A fictitious NEO with $a \leq a_R$ requires MA = 180, and a fictitious NEO with $a > a_R$ requires MA = 0.

A: the value of a in AU specific to the fictitious NEO ephemeris being generated.

OM: J2KE longitude of ascending node in deg. All fictitious NEOs use OM = 0.

W: J2KE argument of perihelion in deg. A fictitious NEO with $a \leq a_R$ requires W = 0, and a fictitious NEO with $a > a_R$ requires W = 180.

IN: the value of i in deg specific to the fictitious NEO ephemeris sequence being generated.

Each Earth and fictitious NEO ephemeris assessed under NHATS constraints starts at 31.0 December 2014 CT and ends at 2.0 January 2042 CT. These ephemerides consist of geometric J2KE positions at 2-day intervals, covering all NHATS-permissible Earth departure and Earth return dates.

Noteworthy HSF accessibility consequences arise from the foregoing J2KE elements defining USSBs to *Horizons*. First, all fictitious NEOs, whether inferior or superior, are "in-phase" with Earth at the initialization epoch such that the condition $\theta = 0$ is imposed. Second, the initialization epoch always coincides with the fictitious NEO heliocentric apsis passage closer to a_R (aphelion for $a \leq a_R$ orbits; perihelion for $a > a_R$ orbits). Consistent with the previously documented accessibility theory, these two conditions ensure each fictitious NEO undergoes one of the most favorable accessibility seasons possible in its orbit. Furthermore, this season falls near the initialization epoch, approximately midway through the NHATS EDI. The season is therefore unlikely to be curtailed by assessment time limits. In this manner, a "level playing field" is created on which each fictitious NEO is equally favored to tally its highest possible n .

Maintaining Fictitious NEO Orbit Classification With Conic Heliocentric Ephemerides

Consider a fictitious NEO sequence consisting of 21 cases whose 20.5 March 2028 CT initialization epoch (a, e, i) coordinates progress according to the series (0.90 AU, 0.05, 0), (0.91 AU, 0.05, 0), ..., (1.09 AU, 0.05, 0), (1.10 AU, 0.05, 0). At the initialization epoch, this sequence of coordinates fully spans the theorized NEAR at $e = 0.05$. Table 4 lists a values among these initialization coordinates, together with the corresponding heliocentric phasing behavior relative to Earth and the resulting n accompanied by its rank within the $(a, 0.05, 0)$ sequence. Table 4 data reflect exported USSB ephemerides generated by *Horizons* with an SDM pedigree.

Table 4. NHATS Fictitious NEO Assessments at $(a, 0.05, 0)$.

Initialization a (AU)	Earth-Relative Phasing from 2015 through 2041	n /Rank
0.90	Atira (0.8988 AU $< a \leq$ 0.9000 AU)	1,426,368/19
0.91	Atira (0.9075 AU $< a \leq$ 0.9100 AU)	1,594,970/18
0.92	Atira (0.9179 AU $< a \leq$ 0.9200 AU)	1,385,650/20
0.93	Atira (0.9287 AU $< a \leq$ 0.9300 AU)	1,681,623/17
0.94	Apollo until January 2028; Aten thereafter	2,326,324/13
0.95	Geocentric distance $< \sim$ 250,000 km	42,954,445/1
0.96	Aten (0.9600 AU $\leq a <$ 0.9800 AU)	1,941,575/16
0.97	Aten (0.9700 AU $\leq a <$ 0.9780 AU)	2,072,537/15
0.98	Aten (0.9798 AU $< a <$ 0.9846 AU)	2,966,543/8
0.99	Aten (0.966 AU $< a <$ 0.996 AU)	4,845,413/6
1.00	Semi-periodic Aten/Apollo transitions (0.997 AU $< a <$ 1.003 AU)	30,826,237/3
1.01	Apollo until June 2030; Aten thereafter	5,128,242/5
1.02	Apollo (1.0121 AU $< a \leq$ 1.0200 AU)	3,581,938/7
1.03	Apollo (1.0147 AU $< a \leq$ 1.0300 AU)	2,786,993/11
1.04	Aten until May 2027; Apollo until July 2027; Aten until February 2028; Apollo thereafter	5,220,894/4
1.05	Geocentric distance $< \sim$ 250,000 km	42,855,048/2
1.06	Apollo until May 2028; Aten thereafter	2,870,959/10
1.07	Amor (1.0695 AU $< a <$ 1.0795 AU)	2,895,089/9
1.08	Amor (1.0772 AU $< a <$ 1.0845 AU)	2,488,575/12
1.09	Amor (1.0897 AU $< a <$ 1.0922 AU)	2,096,862/14
1.10	Amor (1.1000 AU $\leq a <$ 1.1015 AU)	1,191,512/21

As noted previously, many catalogued NEOs possess dynamic (a, e, i) coordinates over time intervals of months or less. Because of their Earth-like orbits, all Table 4 fictitious NEOs see appreciable Earth gravity accelerations from the SDM on one or more occasions. In 7 of these 21 cases, Earth gravity perturbations to the respective heliocentric orbits are sufficient to alter the fictitious NEO's orbit classification at least once between 2015 and 2042.

The cases at $a = 0.95$ AU and $a = 1.05$ AU spend the entire NHATS EDI in elliptic geocentric orbits well inside the Moon's. Although these cases have n tallies approaching 43 million NHATS-compliant solutions, likely near the maximum theoretically possible, they are nevertheless dynamically nonsensical. Fictitious NEO initialization intentionally results in nearly the closest possible Earth encounter for the

specified (a, e, i) coordinates at the 20.5 March 2028 CT initialization epoch. Consequently, these two cases never gain kinetic energy by falling toward Earth from interplanetary space. Instead, they "materialize" inside the Moon's orbit with insufficient geocentric speed to depart Earth's vicinity.

Due chiefly to Earth gravity modeling by *Horizons'* SDM in USSB fictitious NEO ephemerides, Table 4 data fail to represent a controlled experiment in NEO accessibility, for which cases with reasonably fixed (a, e, i) coordinates are required. Even among the 14 cases remaining in one orbit classification throughout the NHATS EDI, considerable overlap in a exists between some cases during this interval. Given the presence of Earth gravity perturbations, it is remarkable that all Table 4 cases remain within $0.008 < e < 0.32$ and $i < 2.9^\circ$ envelopes during the NHATS EDI. Limits for both envelopes are only approached by the aberrant (0.95 AU, 0.05, 0) and (1.05 AU, 0.05, 0) cases.

The solution eliminating experimental chaos due to Earth gravity perturbations is straightforward. If fictitious NEO ephemerides with a heliocentric conic trajectory pedigree are generated, static (a, e, i) coordinates are imposed. When first considered, this solution appears flawed by its blatant departure from real world dynamics, particularly for highly accessible fictitious NEOs undergoing close Earth encounters. But this departure is largely irrelevant to study of relative accessibility among NEOs. While it is true that near-captures of NEOs like 2003 YN₁₀₇ by Earth are not possible with conic fictitious NEO ephemerides, such cases are rare and confined to the programmatically unfavorable (a, e, i) region near (1 AU, 0, 0). Close Earth encounters are still possible without Earth gravity modeling, and simulated missions with the loiter segment conducted well within Earth's gravitational sphere of influence will produce optimistic accessibility results. Such missions are also rare, and only those targeting NEO destinations with relatively small n would fail to remain NHATS-compliant if Earth gravity were to be modeled. Earth gravity is largely irrelevant to the spacecraft trajectory in close Earth encounter cases because outbound and return segments traverse short geocentric distances.

As an illustration of heliocentric conic fictitious NEO ephemerides applied to NHATS, consider the formerly problematic case with initial (a, e, i) coordinates (0.95 AU, 0.05, 0). Table 5 lists conic ephemeris geocentric distance values for this case at standard NHATS ephemeris epochs and at the fictitious NEO initialization epoch. The time interval spanned by Table 5 is during the only Earth approach of this conic fictitious NEO closer than 0.1 AU throughout the NHATS EDI.

Table 5. Earth Close Approach by Conic Fictitious NEO Ephemeris at (0.95 AU, 0.05, 0).

Epoch (CT)	Geocentric Distance (km)
8.0 March 2028	1,151,673
10.0 March 2028	990,663
12.0 March 2028	830,224
14.0 March 2028	670,908
16.0 March 2028	514,627
18.0 March 2028	366,959
20.0 March 2028	246,247
20.5 March 2028	225,816
22.0 March 2028	208,334
24.0 March 2028	288,127
26.0 March 2028	423,039
28.0 March 2028	574,632
30.0 March 2028	731,669
1.0 April 2028	890,454
3.0 April 2028	1,049,654

In the NHATS context, a fictitious NEO ephemeris provides Lambert boundary values, together with velocities permitting Δv_A and Δv_D to be computed. If this ephemeris fails to account for Earth gravity, its function is not significantly compromised. Even in the rare case of a close Earth approach well inside the Moon's orbit, Table 5 indicates the period of significant geocentric speed errors is measured in weeks. Consequently, all fictitious NEO accessibility data presented hereinafter reflect Reference 6 heliocentric conic trajectory modeling using μ_S and *Horizons* J2KE initial conditions.

Smoothing n Versus a For Fictitious NEOs In Period-Resonant Orbits With Earth's

Assessments under NHATS demonstrate that heliocentric conic fictitious NEO orbits in period resonances with Earth's orbit can strongly influence n . Local maxima in n as a function of a arise consistently in resonant cases because of the in-phase $\theta = 0$ condition imposed on each fictitious NEO at the initialization epoch. With this epoch selected about midway through the 26-year NHATS EDI, any resonant case with $t_S < 13$ years will be in-phase with Earth at least three times during that interval. As previously noted, any relatively accessible NEO will tend to tally copious NHATS-compatible trajectory solutions whenever it is nearly in-phase with Earth.

The a value corresponding to exactly j heliocentric revolutions completed by a NEO during the same t_S in which Earth completes exactly k heliocentric revolutions is easily computed according to Equations (14) and (15). This condition is termed a $j : k$ resonance. For reference purposes, Tables 6a and 6b contain resonant a values in AU for $0 < j < 13$ and $0 < k < 13$.

$$\omega = \frac{j \omega_R}{k} \quad (14)$$

$$a = \left[\frac{\mu_S}{\omega^2} \right]^{1/3} \quad (15)$$

Table 6a. a Values in AU Leading to $j < 13 : k < 7$ NEO Resonances with Earth.

j	k					
	1	2	3	4	5	6
1	1	1.5874010	2.0800838	2.5198421	2.9240177	3.3019272
2	0.6299605	1	1.3103706	1.5874010	1.8420157	2.0800838
3	0.4807498	0.7631428	1	1.2114137	1.4057211	1.5874010
4	0.3968502	0.6299605	0.8254818	1	1.1603972	1.3103706
5	0.3419951	0.5428835	0.7113786	0.8617738	1	1.1292432
6	0.3028534	0.4807498	0.6299605	0.7631428	0.8855488	1
7	0.2732758	0.4337984	0.5684367	0.6886120	0.7990635	0.9023370
8	0.25	0.3968502	0.5200209	0.6299605	0.7310044	0.8254818
9	0.2311204	0.3668808	0.4807498	0.5823869	0.6758002	0.7631428
10	0.2154434	0.3419951	0.4481404	0.5428835	0.6299605	0.7113786
11	0.2021800	0.3209407	0.4205513	0.5094616	0.5911779	0.6675836
12	0.1907857	0.3028534	0.3968502	0.4807498	0.5578607	0.6299605

Table 6b. a Values in AU Leading to $j < 13 : 6 < k < 13$ NEO Resonances with Earth.

j	k					
	7	8	9	10	11	12
1	3.6593057	4	4.3267487	4.6415888	4.9460874	5.2414827
2	2.3052181	2.5198421	2.7256808	2.9240177	3.1158398	3.3019272
3	1.7592106	1.9229994	2.0800838	2.2314431	2.3778308	2.5198421
4	1.4521964	1.5874010	1.7170713	1.8420157	1.9628561	2.0800838
5	1.2514649	1.3679807	1.4797272	1.5874010	1.6915381	1.7925618
6	1.1082332	1.2114137	1.3103706	1.4057211	1.4979395	1.5874010
7	1	1.0931035	1.1823960	1.2684342	1.3516464	1.4323708
8	0.9148264	1	1.0816871	1.1603972	1.2365218	1.3103706
9	0.8457402	0.9244816	1	1.0727659	1.1431418	1.2114137
10	0.7883735	0.8617738	0.9321697	1	1.0656022	1.1292432
11	0.7398384	0.8087200	0.8747820	0.9384364	1	1.0597230
12	0.6981432	0.7631428	0.8254818	0.8855488	0.9436427	1

Figure 6 is an n versus a plot for an $(a, 0.10, 0)$ fictitious NEO sequence spanning the theorized NEAR and covering the 26-year NHATS EDI. Correlation between annotated resonant conditions in this plot and local maxima in n is highly evident. This plot is also annotated with a values satisfying $t_S = 25$ years, together with GReMS and ZePHA conditions at $e = 0.10$. Figure 6 local maxima in n can be turned into local minima simply by initializing fictitious NEOs such that $MA = 0$ for $a \leq a_R$ and $MA = 180$ for $a > a_R$, while initializing $W = 180$ for $a \leq a_R$ and $W = 0$ for $a > a_R$. Excepting the 1 : 1 resonance maximum, all extrema in the $(a, 0.10, 0)$ sequence can be suppressed by collapsing the NHATS EDI from 26 years to the 5 years centered on the fictitious NEO initialization epoch. In this manner, even Figure 6 resonances with the smallest $k > 1$ (6 : 5 and 4 : 5) cannot achieve a $\theta = 0$ in-phase condition other than at the fictitious NEO initialization epoch.

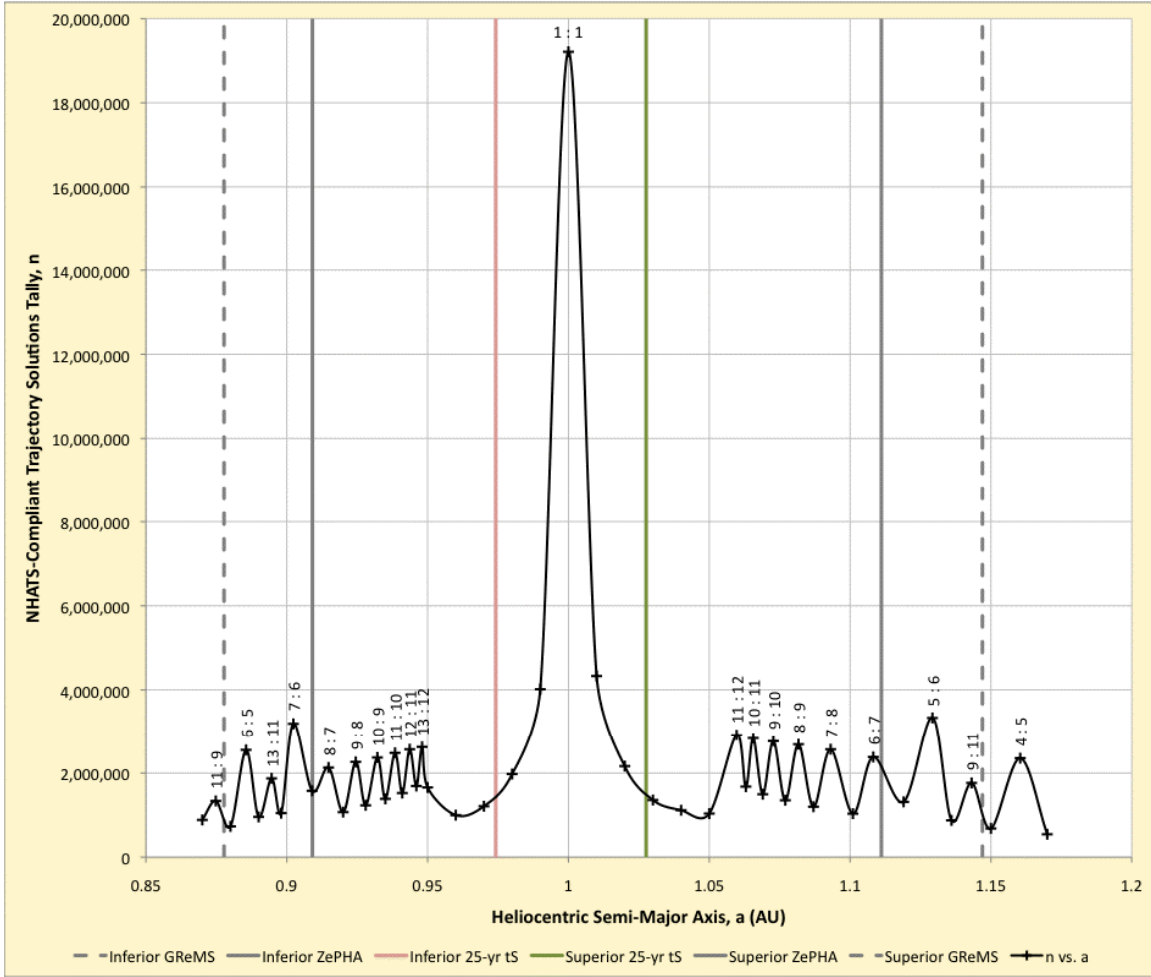


Figure 6. A 26-Year EDI n Versus a Plot for the Fictitious NEO Sequence at $(a, 0.10, 0)$.

Smoothing effects of the 5-year EDI on the n versus a plot at $(a, 0.10, 0)$ are evident in Figure 7. This smoothing permits more critical accessibility comparisons between inferior and superior fictitious NEOs at similar t_S , also equivalent to resonant cases at the same k when $|j - k| = 1$. Enhanced inferior accessibility, expected from theory with respect to equivalent superior cases, is not evident in Figure 7. Additional research will be necessary to reconcile this apparent contradiction.

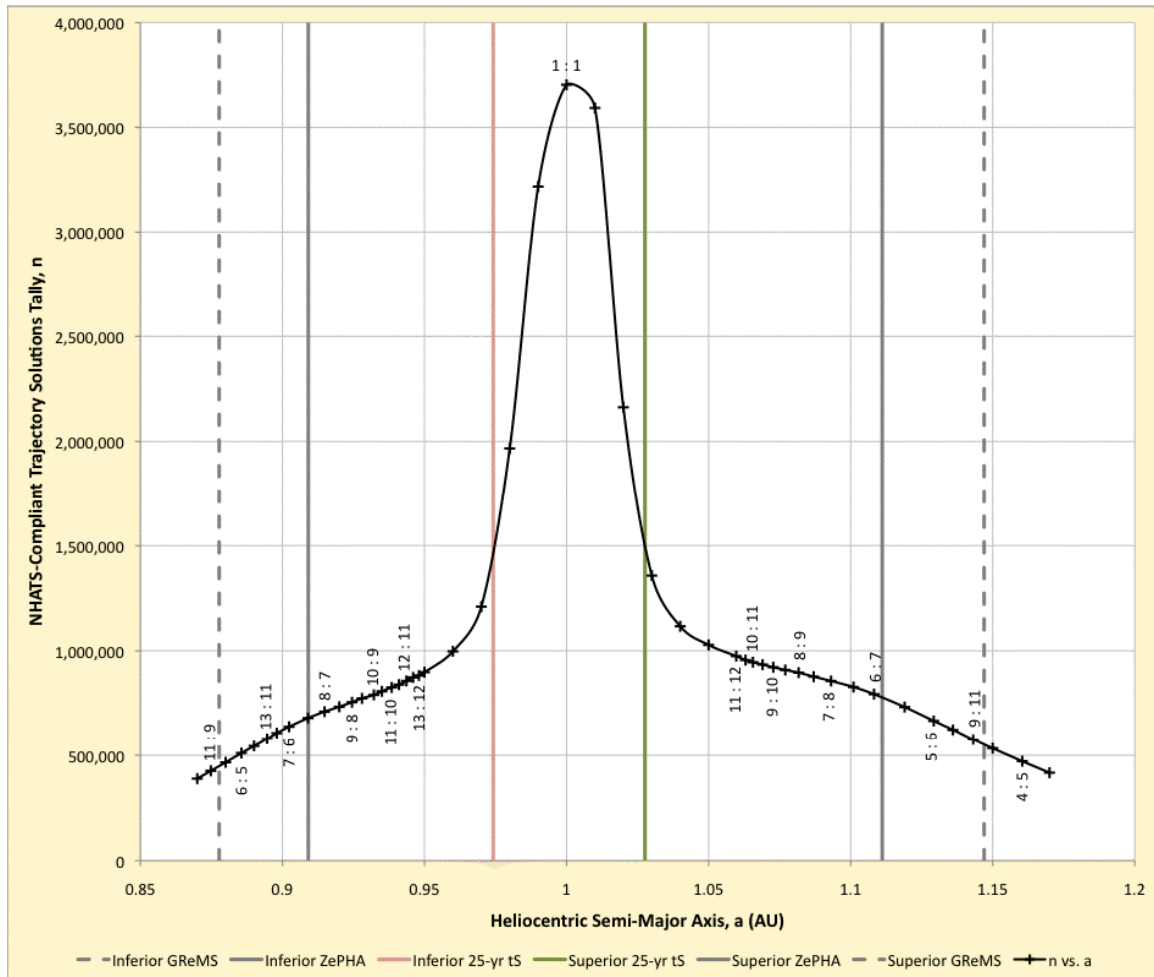


Figure 7. A 5-Year EDI n Versus a Plot for the Fictitious NEO Sequence at $(a, 0.10, 0)$.

CONCLUSIONS

Empirical NHATS-derived evidence has been presented and correlated with a theory identifying regions in heliocentric (a, e, i) space offering relatively high NEO accessibility for HSF. Of the 50 most accessible NEOs according to the NHATS metric n , only 4 (ranked #19, #21, #33, and #40) from the superior Amor orbit classification fail to lie within the theorized NEAR. In addition, no NEO with an n -ranking in the NHATS "top 50" exhibits a t_S significantly greater than the 26-year NHATS EDI during that interval, creating a "programmatic cutout" through the NEAR's central region in an e versus a plot (see Figure 5).

Inferior of the ZePHA condition partially defining the NEAR's inferior boundary, there are no known NEOs at $e < 0.2$ and $i < 10^\circ$ as of epoch 2011.0. Close to the corresponding superior NEAR boundary, members of the Apollo orbit classification enjoy NHATS n -rankings as high as #6, #7, and #8 (see Figure 5). The dearth of inferior NEOs with potentially high accessibility is almost certainly an artifact of attempting to observe them from vantages exclusively near Earth. Knowing inferior NEAR limits in helio-

centric (a, e, i) space can help guide design, deployment, and operation of future NEO survey instrumentation located in deep space.

Ongoing work to corroborate NEO accessibility theory by systematically assessing fictitious NEO sequences has been reported. This work is far from complete and is already known to entail non-intuitive techniques such as heliocentric conic fictitious NEO orbit modeling and a curtailed NHATS EDI. According to HSF accessibility theory, multiple orbit dynamics asymmetries favor an inferior NEO's accessibility with respect to an equivalent superior NEO's. Confirmation of this enhanced accessibility through controlled fictitious NEO assessments awaits additional research. It may be necessary to further modify NHATS destination viability criteria or to perform discrete trajectory design assessments under highly controlled conditions to achieve this confirmation. In discrete designs, assessments would use mission-specific metrics such as Δv or initial mass in low Earth orbit (with an assumed architecture) as substitutes for n .

ACKNOWLEDGMENTS

The authors are indebted to Dr. Lindley Johnson, Program Manager of NASA's Near Earth Objects Observation Program, for his leadership and guidance during the genesis of NHATS. Experiments with fictitious NEOs were enabled through timely and effective *Horizons* software maintenance rendered by Jon Giorgini of JPL's Solar System Dynamics Group.

REFERENCES

- ¹ Adamo, D. R., Giorgini, J. D., Abell, P. A., and Landis, R. R., "Asteroid Destinations Accessible For Human Exploration: A Preliminary Survey in Mid-2009", *Journal of Spacecraft and Rockets*, Vol. 47, No. 6, AIAA, Washington, D.C., 2010, pp. 994-1002.
- ² National Research Council Committee to Review Near-Earth Object Surveys and Hazard Mitigation Strategies, *Defending Planet Earth: Near-Earth Object Surveys and Hazard Mitigation Strategies: Final Report*, The National Academies Press, Washington, D.C., 2010.
- ³ Giorgini, J. D., Yeomans, D. K., Chamberlin, A. B., Chodas, P. W., Jacobson, R. A., Keesey, M. S., Lieske, J. H., Ostro, S. J., Standish, E. M., and Wimberly, R. N., "JPL's On-Line Solar System Data Service," *Bulletin of the American Astronomical Society*, Vol. 28, No. 3, 1996, p. 1158.
- ⁴ Barbee, B. W., Esposito, T., Piñon, E. III, Hur-Diaz, S., Mink, R. G., and Adamo, D. R., "A Comprehensive Ongoing Survey of the Near-Earth Asteroid Population for Human Mission Accessibility", *Proceedings of the AIAA/AAS Guidance, Navigation, and Control Conference 2 - 5 August 2010, Toronto, Ontario Canada*, Paper 2010-8368, AIAA, Washington, D.C., 2010.
- ⁵ Hopkins, J. B. and Dissel, A. F., "Plymouth Rock: An Early Human Mission to Near-Earth Asteroids Using Orion Spacecraft", *Proceedings of the AIAA Space 2010 Conference and Exposition 30 August - 2 September 2010, Anaheim, California*, Paper 2010-8608, AIAA, Washington, D.C., 2010.
- ⁶ Adamo, D. R., "A Precision Orbit Predictor Optimized For Complex Trajectory Operations", *Volume 116 of the Advances in the Astronautical Sciences Series, AAS/AIAA Astrodynamics Conference 2003*, Paper AAS 03-665, Univelt, San Diego, California, 2003.